# Experimental validation of a nonparametric probabilistic model of nonhomogeneous uncertainties for dynamical systems. — **Source link** ⬈

Hamid Chebli, Christian Soize

**Topics:** Dynamical systems theory, Uncertainty quantification and Statistical model

Related papers:

- A nonparametric model of random uncertainties for reduced matrix models in structural dynamics

- Random matrix theory for modeling uncertainties in computational mechanics

- Maximum entropy approach for modeling random uncertainties in transient elastodynamics.

- Probabilistic approach for model and data uncertainties and its experimental identification in structural dynamics: Case of composite sandwich panels

- Transient dynamics in structures with non-homogeneous uncertainties induced by complex joints

Share this paper: 🅕 🐦 in ✉

# Experimental validation of a nonparametric probabilistic model of nonhomogeneous uncertainties for dynamical systems

H. Chebli, Christian Soize

# EXPERIMENTAL VALIDATION OF A NONPARAMETRIC PROBABILISTIC MODEL OF NON HOMOGENEOUS UNCERTAINTIES FOR DYNAMICAL SYSTEMS

Hamid Chebli[1] & Christian Soize[2]

[1] *Structural Dynamics and Coupled Systems Department, ONERA, 92322 Châtillon , France.*

[2] *Laboratoire de Mécanique, Université de Marne-La-Vallée, 77454 Marne-La-Vallée, France.*

**ABSTRACT**

The paper deals with an experimental validation of a nonparametric probabilistic model of non homogeneous uncertainties for dynamical systems. The theory used, recently introduced, allows model uncertainties and data uncertainties to be simultaneously taken into account. An experiment devoted to this validation was specifically developed. The experimental model is constituted of two simple dural rectangular plates connected together with a complex joint. In the mean mechanical model, the complex joint which is constituted of two additional plates attached with 40 screw-bolts, is modeled by a homogeneous orthotropic continous plate with constant thickness, as usual. Consequently, the mean model introduces a region (the joint) which has a high level of uncertainties. The objective of the paper is to present the experiment and the comparisons of the theoretical prediction with the experiments.

**INTRODUCTION**

In order to improve the robustness of the prediction models of complex dynamical systems, random uncertainties have to be taken into account. There are two main types of uncertainties : (1) *model uncertainties* which are induced by the modeling process which allows the mathematical model of the real dynamical systems to be constructed and (2) *data uncertainties* which correspond to the errors on the parameters of the constructed model. It is well known that probabilistic parametric approaches are very efficient to model the data uncertainties (for instance, see Refs. 1 to 7). However, probabilistic approaches do not allow model uncertainties to be taken into account. This is the reason why a nonparametric probabilistic model of random uncertainties for dynamical systems

has recently been proposed[8;9]. This nonparametric approach allows model uncertainties and data uncertainties to be simultaneously taken into account. Without re-explaining all the details of this nonparametric approach, hereafter, we summarize the principal idea. First, it should be noted that any probability measure can be constructed using the maximum entropy principle[9] with appropriate constraints. Consequently, when a probability measure has to be constructed, the problem is to utilize the constraints defined by the better available information. For dynamical systems, the most important available information is relative to the operators of the nominal model (such as the mass, damping and stiffness operators of the nominal model presently called the mean model) and to their algebraic properties. Modeling random uncertainties leads the corresponding operators of the dynamical system to be random and to verify the same algebraic properties (positiveness, invertibility, etc). For the actual dynamical system, the corresponding operators are unknown but it can be state that these operators have to verify the same algebraic properties which are absolutely general for any dynamical system. In addition, for the statistical identification of the predictive model, the actual dynamical system under consideration have to be considered as a realization of a random dynamical system. For a given operator of the predictive model, the probabilistic parametric approach of data uncertainties yields an operator range which is a subset $\mathbb{S}_{par} \subset \mathbb{S}$ of an appropriate functional space $\mathbb{S}$ and which can be too "small" due to the presence of additional model uncertainties. This means that, if the model uncertainties are large, the corresponding operator of the actual dynamical system does not belong to subset $\mathbb{S}_{par}$. The proposed probabilistic nonparametric approach consists in constructing a "bigger subset" $\mathbb{S}_{nonpar}$ using only the known general algebraic properties which hold for any dynamical system. Consequenty, by construction, $\mathbb{S}_{nonpar}$ contains subset $\mathbb{S}_{par}$ (that is to say $\mathbb{S}_{par} \subset \mathbb{S}_{nonpar}$) and then, the operator of the actual dynamical system belongs to $\mathbb{S}_{nonpar}$. Then, a probability measure is constructed on $\mathbb{S}_{nonpar}$ and this is done using the maximum entropy principle with the constraints defined by all the available information related to the given operator of the dynamical system.

In Refs. 8 and 9, the theory is presented for master dynamical systems with homogeneous random uncertainties. Generally, for complex dynamical systems, random uncertainties are not homogeneous. The level of uncertainty is different from a part to another one. For instance, if we consider two simple structures connected together with a complex joint, the uncertainties of the mean mechanical model are important in the part constituted of the joint and are small in the two parts constituted of the two simple structures. Consequently, the nonparametric probabilistic

model of random uncertainties has been extended to the case of non homogeneous uncertainties by using a substructuring technique[10−12]. Such an approach combines the Craig-Bampton dynamic substructuring method[13] and the nonparametric probabilistic model.

In order to validate the nonparametric probabilistic model of non homogeneous uncertainties for complex dynamical systems, an experiment has specifically been carried out[14]. In this paper, we present this experiment and the experimental validation of the theory developed in Refs. 8 to 12 and which constitutes the first experimental validation of the proposed nonparametric probabilistic approach.

The experimental set-up is made up of two dural rectangular plates connected together by a complex joint constituted of two additional plates and 40 screw bolts. Then, the dynamical system has three natural subdomains. The first one is a simple rectangular plate, the second one is a complex joint and the third one is an another simple rectangular plate. In order to evaluate the role played by the value and by the distribution of the screwing-couples, 21 configurations corresponding to 21 values and distributions of the screwing-couples have been tested.

The mean numerical model is constituted of a finite element model of a simplified schematization of the dynamical system for which the complex joint is replaced by an equivalent simple orthotropic continuous plate with constant thickness. The modeling uncertainties are induced by the introduction of such a simple schematization of the complex joint. The finite element model of the orthotropic continuous plate modeling the complex joint has been updated using the first seventh experimental elastic modes. Nevertheless, in spite of this dynamical updating, the mean finite element model cannot correctly predict the frequency response functions on a broad frequency band, especially when the frequency increases. The comparisons of the experimental frequency response functions with the mean finite element model clearly show that the mean model is good for the low-frequency range but is not able to predict the experimental responses for higher frequencies. The introduction of a nonparametric model of non homogeneous random uncertainties allows the robustness of the prediction to be improved.

In Section I, the experimental set-up is presented. Section II deals with the mean mechanical model and its finite element modeling. In Section III, we present the comparisons of the frequency responses given by the mean model with the experimental frequency responses. Section IV is devoted to the comparisons of the random frequency responses of the stochastic model with the experimental frequency responses. Below, FRF means "frequency response function".

## I. EXPERIMENT

The experiment which is briefly described below was performed at ONERA[14]. The system studied is constituted of two simple rectangular thin plates connected by a bolted joint, as explained in Section Introduction.

### A. Description of the experimental set-up

The two simple plates of the experimental system are noted $P_1$ and $P_3$. Plate $P_1$ is a rectangular dural plate with thickness $0.003\ m$, width $0.40\ m$ and lenght $0.60\ m$. Plate $P_3$ is a rectangular dural plate with thickness $0.003\ m$, width $0.50\ m$ and lenght $0.60\ m$. Plates $P_1$ and $P_3$ are connected on their lenght by a joint constituted of two rectangular plates with thickness $0.002\ m$, width $0.14\ m$ and lenght $0.60\ m$ (see Fig. 1) and are attached with two lines of 20 screw-bolts. The experimental dynamical system is hanged with a very low eigenfrequency. The excitation is done with an electrodynamic shaker located in plate $P_3$ (see $k_{exit}$ in Fig. 1). The response is identified with 29 accelerometers. Below, we present experimental measurements for the two accelerometers located at point $k_{exit}$ (driving force) in plate $P_3$ and at point $k_{obs}$ in plate $P_1$ (see Fig. 1).

### B. Experimental configurations

In order to study the influence of the screw-bolt prestresses, 21 experimental configurations were defined. Each experimental configuration corresponds to a given value of each screw-bolt prestress for the 40 screw-bolts. The prestresses of these 40 screw-bolts correspond to the realization of a random screwing-couple of each screw-bolt. The probability distribution is uniform on the interval $[2,5]N \times m$. The 21 experimental configurations were tested.

### C. Experimental measurements

For each experimental configuration $j = 1, \ldots, 21$, the data collected are the accelerations $\{A_k^{\mathrm{exp},j}(f), k = 1, \ldots, 29\}$, for $f$ in $B = [20, 2000]\ Hz$. From the measured accelerations, the displacements $U_k^{\mathrm{exp},j}(f)$ are easily deduced. For each $f$ in $B$, we introduce the functions $f \mapsto \mathrm{Max}_k^{\mathrm{exp}}(f)$ and $f \mapsto \mathrm{Min}_k^{\mathrm{exp}}(f)$ related to the 21 experimental configurations and defined by

$$\mathrm{Max}_k^{\mathrm{exp}}(f) = \max_{j=1,\ldots,21}\{10\log_{10}(|U_k^{\mathrm{exp},j}(f)|^2)\}, \tag{1}$$

$$\text{Min}_k^{\text{exp}}(f) = \min_{j=1,...,21} \{10 \log_{10}(|U_k^{\text{exp},j}(f)|^2)\}. \qquad (2)$$

## D. Influence of the screw-bolt prestresses

Figure 2 displays the experimental results of the displacement FRF modulus for observation point $k_{obs}$ in plate $P_1$. The upper and lower curves correspond to the graphs of functions $f \mapsto \text{Max}_{k_{obs}}^{\text{exp}}(f)$ and $f \mapsto \text{Min}_{k_{obs}}^{\text{exp}}(f)$ respectively. It can be seen that the dispersion induced by the random screw-bolt prestresses is completely negligible in the $[0, 200]Hz$ frequency band, is small in $[200, 800]Hz$ and is still limited in the $[800, 2000]Hz$ frequency band. It can be concluded that the screw-bolt prestresses induce a small dispersion which is increasing with the frequency.

## II. MEAN MECHANICAL MODEL OF THE EXPERIMENTAL CONFIGURATIONS

This Section deals with the construction of the mean mechanical model of the experimental configurations and with the updating of the finite element model.

### A. Mean mechanical model

We consider the complete structure $\Omega$ whose dimension is $0.9\ m \times 0.6\ m$ in a Cartesian coordinate system (O X Y Z) defined in Fig. 3. This structure is constituted of three substructures $\Omega^1$ (plate $P_1$), $\Omega^2$ (joint) and $\Omega^3$ (plate $P_3$), whose lenghts are $0.33\ m$, $0.14\ m$ and $0.43\ m$ respectively. The thickness of substructures $\Omega^1$ and $\Omega^3$ is $0.003\ m$. The joint is modeled by substructure $\Omega^2$ whose thickness is $0.007\ m$ (corresponding to $0.002 + 0.003 + 0.002$, see Fig. 3). The coupling interface between $\Omega^1$ and $\Omega^2$ is $\Sigma^1$, and between $\Omega^2$ and $\Omega^3$ is $\Sigma^2$.

Plates $P_1$ (substructure $\Omega^1$) and $P_3$ (substructure $\Omega^3$) are made in dural and consequently are modeled by a homogeneous isotropic material whose measured characteristics are the following: mass density $2800\ kg/m^3$, Young's modulus $7.05 \times 10^{10}\ N/m^2$, Poisson's rate $0.33$ and damping rate $0.2\%$. If the joint (substructure $\Omega^2$) is modeled by a homogeneous and isotropic plate with thickness $0.007\ m$, then the seven lowest eigenvalues of the structure $\Omega$ can never been predicted with a sufficient accuracy when the prediction is compared with the experiments. It can be concluded that an orthotropic medium is required for the mean model of the joint. Such an orthotropic model was developed and the characteristic properties were identified by updating the finite element model

(see Section II.C). The mass of each accelerometer ($0.0007kg$) is introduced in the model. An appropriate system of four springs models the experimental hanging.

The modal damping rates have been experimentally identified for the ten first elastic modes. The mean value of these experimental damping rates is $0.2\%$. For the mean damping of each sub-structure, a hysteretic model is used. Consequently, the mean damping matrix of each substructure is proportional to the mean stiffness matrix with a coefficient equal to $2\beta/(2\pi f)$ in which $\beta = 0.002$ and where $f$ is the frequency in Hz.

The coordinates of excitation point $k_{exit}$ are $(0.77, 0.45, 0)$. In the frequency domain, the driving force is a constant normal force applied to the plate $P_3$ (substructure $\Omega^3$) over frequency band $B$ and is equal to $1$. The normal displacement at points $k_{exit}$ and $k_{obs}$ (corresponding to the location of two accelerometers) are observed to characterize the dynamical responses of structure $\Omega$. The coordinates of observation point $k_{obs}$ are $(0.09, 0.36, 0)$.

## B. Mean finite element model of the experimental configurations

The mean finite element models of the three substructures $\Omega^1$, $\Omega^2$ and $\Omega^3$ are constructed with compatible meshes constituted of 4-nodes bending plate elements. The mesh size is $0.01\,m \times 0.01\,m$. The assembled structure $\Omega$ has 16653 DOFs, the number of internal DOFs of $\Omega^1$ (plate $P_1$), $\Omega^2$ (joint) and $\Omega^3$ (plate $P_3$) is 6039, 2379 and 7869 respectively. The number of coupling DOFs for each interface $\Sigma^1$ and $\Sigma^2$ is 183. The observation DOFs corresponding to the normal displacement at driving point $k_{exit}$ and at observation point $k_{obs}$ are noted $\mathrm{dof}_{exit}$ and $\mathrm{dof}_{obs}$ respectively (see Fig. 3).

## C. Properties of the mean model

The mesh size of the mean finite element model has been adapted to the wave numbers of the highest mode in the frequency band $B = [0\,,2000]$ Hz of analysis. The modal density of the mean structure is such that there are 8 modes in the frequency band $[20\,,100]$ Hz, 27 modes in $[100\,,500]$ Hz, 29 modes in $[500\,,1000]$ Hz, 33 modes in $[1000\,,1500]$ Hz and finally, 29 modes in $[1500\,,2000]$ Hz. For the mode corresponding to the highest eigenfrequency in frequency band $B$ (the highest mode), the corresponding wave numbers $n$ and $m$ in $X$ and $Y$ directions (see Fig. 3) are $n = 15$ and $m = 10$. Since mean finite element mesh is such that there are 90 finite element nodes in $X$ and direction and 60 finite element nodes in $Y$ direction, the spatial sampling for the highest mode is 6 nodes per "half wavelength" in each direction. Consequently, the mean finite element mesh is

sufficiently refined to give converged results in the sense of the mean model.

**D. Updating the mean finite element model**

In order to improve the quality of the mean finite element model, the mean finite element model of the joint (substructure $\Omega^2$) has been updated with respect to the seven lowest eigenfrequencies which have been measured. The updated model for substructure $\Omega^2$ corresponds to an orthotropic material whose Young's moduli are $E_X = 1.90 \times 10^{10}\ N/m^2$ and $E_Y = 7.40 \times 10^{10}\ N/m^2$ and whose in-plane shear modulus is $1.23 \times 10^{10}\ N/m^2$. Moreover, the mass of each screw-bolt is taken into account and the resulting mass density of substructure $\Omega^2$ is equal to $3086\ kg/m^3$. The seven lowest experimental eigenfrequencies are 20.35 Hz, 22.12 Hz, 37.97 Hz, 52.80 Hz, 57.99 Hz, 66.58 Hz and 84.70 Hz, while the calculated eigenfrequencies with the updated mean finite element model are 20.35 Hz, 22.54 Hz, 40.25 Hz, 53.32 Hz, 57.10 Hz, 66.36 Hz and 84.02 Hz.

**III. RESPONSE OF THE MEAN MODEL AND COMPARISONS WITH THE EXPERIMENTAL RESULTS**

In this Section, the response of the mean model calculated by using the Craig-Bampton dynamic substructuring method is compared with the experimental results. Figures 4 and 5 are related to the driving point $k_{exit}$ and to the observation point $k_{obs}$ respectively. Each figure is relative to the FRF modulus in dB for the displacement and compares the mean numerical predictions with the experimental upper and lower envelopes. Although the updating of the mean finite element model using the experiments has been carried out, for frequencies greater than 400 Hz, Figures 4 and 5 clearly show that the updated mean model is not sufficiently accurate to predict the experimental response for frequencies greater than $400 Hz$. Figures 7 and 9 can be used as a zoom (magnified figures) for studying frequencies less than 400 Hz and show that, in fact, the updated mean finite element model is not sufficiently accurate to predict the experimental response for frequencies greater than $100 Hz$. It should be noted that the number of DOFs for such a system is relatively high with respect to the usual state of art for this type of finite element modeling. Since the effect of the screwing couple is under control through the experimental configurations, it is clear that the main source of uncertainty does not come from this phenomena, but from the model errors (model uncertainties) whose effects increase with frequency (errors induced by the schematization used for modeling a complex joint by a simple continuous plate). Data errors (data uncertainties) exist as well.

## IV. NONPARAMETRIC MODEL OF NON HOMOGENEOUS RANDOM UNCERTAINTIES AND COMPARISONS WITH THE EXPERIMENTAL RESULTS

As explained in Section III, a model uncertainties associated with the mean model constructed in Section II have to be taken into account to increase the robustness of the prediction due to the unsatisfaying prediction given by the mean model. The dispersion parameter $\delta$ which allows the nonparametric probabilistic model to be controled is defined in Ref. 9 and is a dimensionless parameter belonging to interval $[0, 1]$. Such a parameter is similar to the variation index in statistics ($\delta = 0$ corresponds to no uncertainties and $\delta = 1$ to the biggest possible level of uncertainty). Moreover, the level of uncertainty is more important in the substructure modeling the joint. In order to model such non homogeneous random uncertainties, the nonparametric probabilistic method proposed in Refs. 10 to 12 is used.

Althought the goal of this paper is not to present some methods for identifying $\delta$ parameters, hereinafter, we summarize the principle possible methods: (i) Since such a nonparametric model of random uncertainties allows model errors to be taken into account, $\delta$ parameters can be used as global parameters to carry out a sensitivity analysis with respect to the model errors and data errors. With such an approach, $\delta$ is not fixed but has to belong to an interval. This method has been used in this paper for calibrating the values of $\delta$ parameters for the two plates and for the joint. (ii) A second method consists in peforming an experimental identification using an appropriate inverse method. Such a research is in progess. (iii) A third method consists in calibrating $\delta$ parameters by using a parametric approach. An example of such a method is given in Ref. 15. (iv) A fourth method consists in constructing an estimation of $\delta$ for a given type of substructures (for instance for a given type of joints) using any one of the two above methods.

### A. Definition of the uncertainty level

A sensitivity analysis has been carried out with respect to the dispersion parameters $\delta_M$, $\delta_D$ and $\delta_K$ related to the mass, damping and stiffness uncertainties in each substructure. Concerning the details of this analysis, we refer the reader to Ref. 10. From this analysis, it can be deduced that a low level of uncertainties has to be introduced in substructures $\Omega_1$ and $\Omega_3$, and a high level of uncertainties has to be used for substructure $\Omega_2$ modeling the joint. Since the mass distribution of the mean model is relatively well known (with respect to frequency band $B$), we have taken $\delta_{M^1} = \delta_{M^2} = \delta_{M^3} = 0$ for the three substructures. Finally, the optimal values for the $\delta_D$ and

$\delta_K$ parameters (corresponding to a confidence region of the stochastic response associated with a probability of 0.95) are $\delta_{D^1} = \delta_{D^3} = 0.10$, $\delta_{D^2} = 0.80$, and $\delta_{K^1} = \delta_{K^3} = 0.15$, $\delta_{K^2} = 0.80$. These values correspond to a high level of uncertainties in substructure $\Omega^2$ (the joint) for the stiffness and the damping. Since the mass of the mean model is updated with the experiment, no significant errors exist for the mass. It should be noted that if a moderate level of uncertainty is considered for substructure $\Omega^2$, then it is not sufficient to obtain a confidence region in which the experimental results are. In addition, it seems to be inconsistent to increase the level of uncertainty in substructures $\Omega^1$ and $\Omega^3$ modeling plates $P_1$ and $P_3$, but substructure $\Omega^2$ has to be considered with a high level of uncertainty.

## B. Comparisons calculation-measurement

Let $\mathbf{U}(f) = \big(U_1(f), \ldots, U_n(f)\big)$ be the random response of struture $\Omega$. A confidence region, constructed by using the Tchebychev inequality, is defined by the upper and lower envelopes $f \mapsto dB_k^+(f)$ and $f \mapsto dB_k^-(f)$ of the FRF modulus in dB for the displacement and corresponding to a given probability level $P_c$ such that

$$P\{dB_k^-(f) < dB_k(f) < dB_k^+(f)\} \geq P_c \quad , \tag{3}$$

in which the random variable $dB_k(f)$ is defined by $dB_k(f) = 10\,log_{10}(|U_k(f)|^2)$ and where the lower envelope $dB_k^-(f)$ and the upper envelope $dB_k^+(f)$ are such that

$$dB_k^-(f) = 2dB_k^0(f) - dB_k^+(f) \quad , \tag{4}$$

$$dB_k^0(f) = 20\,\log_{10}(|E\{U_k(f)\}|) \quad , \tag{5}$$

$$dB_k^+(f) = 20\,log_{10}\left\{|E\{U_k(f)\}| + a_k(f)\right\} \quad , \quad a_k(f) = \frac{\sigma_{U_k(f)}}{\sqrt{1 - P_c}} \quad , \tag{6}$$

in which $E\{U_k(f)\}$ and $\sigma_{U_k(f)}$ are the mean value and the standard deviation of the complex-valued random variable $U_k(f)$. Figures 6 to 9 display the comparisons between the experiment and the prediction. It should be noted that the mean value $E\{U_k(f)\}$ and the standard deviation $\sigma_{U_k(f)}$ can easily be deduced from Eqs. (4)-(6). Figures 6 and 7 are relative to the displacement at driving point $k_{exit}$ over frequency band $[20, 2000]Hz$ (see Fig. 6) and $[20, 1000]Hz$ (zoom given by Fig. 7). Figure 8 and 9 are relative to the displacement at observation point $k_{obs}$ over frequency band $[20, 2000]Hz$ (see Fig. 8) and $[20, 1000]Hz$ (zoom given by Fig. 9). On each figure, it can be seen (1) the gray region whose upper and lower envelopes are defined by the graphs $f \mapsto dB_k^+(f)$

and $f \mapsto dB_k^-(f)$ and which corresponds to the confidence region with $P_c = 0.95$, constructed using the probabilistic numerical model, (2) the thick solid line corresponding to the response of the mean finite element model and (3) the upper and lower thin solid lines corresponding to the upper and lower envelopes of the experimental FRF for the displacements. It can be seen that the gray region contains almost all the experimental results (in the $0.95$ probability) and that the bandwith of this region increases with the frequency. This is consistent with the fact that the role played by uncertainties increase with the frequency.

In order to explain the efficiency of the proposed nonparametric probabilistic method of non homogeneous model uncertainties, we focuss the analysis given below on a particular aspect of this experimental comparison. Let us consider the resonance predicted by the mean finite element model at frequency $660Hz$ (see the peak of the thick solid line in Fig. 7). The corresponding experimental resonance is given at frequency $628Hz$ (see the peak of the upper and the lower thin solid lines in Fig. 7). If the mean model was perfectly correct, these two resonances should be loacted at the same frequency. It is not the case. It can be seen that the gray region is not centered around the response of the mean finite element model but is shifted allowing the confidence region to include the experimental resonance at $628Hz$. Such an analysis can be reproduced for almost all the differences appearing between the experimental results and the prediction over all the frequency band.

## V. CONCLUSIONS

We have presented an experimental validation of the nonparametric model of random uncertainties proposed in Ref. 9 for the case of non homogeneous uncertainties induced by a complex joint. The experimental comparisons show the efficiency of the theory proposed and show that such a theory has to predict a confidence region which has to increase with the frequency, that is the case for this theory. Finally, this paper shows that, in a broad low-frequency range, the use of such a nonparametric probabilistic model allows the dynamical responses of a structure including a complex joint to be predicted by using a usual mean mechanical model of the joint.

## ACKNOWLEDGEMENTS

[1] E. J. Haug, K. K. Choi and V. Komkov, *Design Sensitivity Analysis of Structural Systems* (Academic Press, 1986).

[2] R. A. Ibrahim, "Structural dynamics with parameter uncertainties", Applied Mechanics Reviews **40**(3), 309-328 (1987).

[3] E. Vanmarcke and M. Grigoriu, "Stochastic finite element analysis of simple beams", Journal of Engineering Mechanics **109**(5), 1203-1214 (1983).

[4] M. Shinozuka and G. Deodatis, "Response variability of stochastic finite element systems", Journal of Engineering Mechanics **114**(3), 499-519 (1988).

[5] P. D. Spanos and R. G. Ghanem, "Stochastic finite element expansion for random media", ASCE Journal of Engineering Mechanics, **115**(5), 1035-1053 (1989).

[6] R. G. Ghanem and P. D. Spanos, *Stochastic Finite Elements: A Spectral Approach* (Springer-Verlag, New York, 1991).

[7] M. Kleiber, D. H. Tran and T. D. Hien, *The Stochastic Finite Element Method* (John Wiley and Sons, 1992).

[8] C. Soize, "A nonparametric model of random uncertainties for reduced matrix models in structural dynamics", Probabilistic Engineering Mechanics, **15**(3), 277-294 (2000).

[9] C. Soize, "Maximum entropy approach for modeling random uncertainties in transient elastodynamics", Journal of the Acoustical Society of America, **109**(5), 1979-1996 (2001).

[10] H. Chebli, *Modélisation des incertitudes aléatoires non homogènes en dynamique des structures pour le domaine des basses fréquences*, (Thèse de doctorat du Conservatoire National des Arts et des Métiers, 2002).

[11] C. Soize and H. Chebli , "Random uncertainties model in dynamic substructuring using a nonparametric probabilistic model", ASCE Journal of Engineering Mechanics, **129**(4),449-457 (2003).

[12] H. Chebli and C. Soize, "Analyse vibratoire par sous-structuration avec modèle non paramétrique d'incertitudes aléatoires non homogènes", Revue européenne des éléments finis, **11**, 234-246 (2002).

[13] R.R.Jr. Craig and M.C.C. Bampton, "Coupling of substructures of dynamic analyses", AIAA Journal, **14**(11), 1313-1319 (1968).

[14] M. Menelle and P. Baroin, ONERA Technical Report RT 1/05809 DDSS (2001) .

[15] C. Soize, "Random matrix theory and non-parametric model of random uncertainties", Journal of Sound and Vibration, **263**, 893-916 (2003).

## LEGENDS ACCOMPANYING EACH FIGURE

FIG. 1. Experimental mechanical system.

FIG. 2. Experimental frequency response function at observation point $k_{obs}$: graphs of functions $f \mapsto \operatorname{Max}_{k_{obs}}^{\exp}(f)$ (upper solid line) and $f \mapsto \operatorname{Min}_{k_{obs}}^{\exp}(f)$ (lower solid line).

FIG. 3. Mean mechanical model of the experimental mechanical system.

FIG. 4. Experimental comparisons at driving point $k_{exit}$ over frequency band $[20, 2000]Hz$: numerical prediction of the frequency response function modulus in dB (thick solid line) and, experimental graphs of $f \mapsto \operatorname{Max}_{k_{exit}}^{\exp}(f)$ (upper thin solid line) and $f \mapsto \operatorname{Min}_{k_{exit}}^{\exp}(f)$ (lower thin solid line).

FIG. 5. Experimental comparisons at observation point $k_{obs}$ over frequency band $[20, 2000]Hz$: numerical prediction of the frequency response function modulus in dB (thick solid line) and, experimental graphs of $f \mapsto \operatorname{Max}_{k_{obs}}^{\exp}(f)$ (upper thin solid line) and $f \mapsto \operatorname{Min}_{k_{obs}}^{\exp}(f)$ (lower thin solid line).

FIG. 6. Experimental comparisons at driving point $k_{exit}$ over frequency band $[20, 2000]Hz$: confidence region prediction in dB with the probabilistic numerical model (gray region), numerical prediction in dB of the mean model (thick solid line) and experimental graphs of $f \mapsto \operatorname{Max}_{k_{exit}}^{\exp}(f)$ (upper thin solid line) and $f \mapsto \operatorname{Min}_{k_{exit}}^{\exp}(f)$ (lower thin solid line).

FIG. 7. Experimental comparisons at driving point $k_{exit}$ over frequency band $[20, 1000]Hz$: confidence region prediction in dB with the probabilistic numerical model (gray region), numerical prediction in dB of the mean model (thick solid line) and experimental graphs of $f \mapsto \operatorname{Max}_{k_{exit}}^{\exp}(f)$ (upper thin solid line) and $f \mapsto \operatorname{Min}_{k_{exit}}^{\exp}(f)$ (lower thin solid line).

FIG. 8. Experimental comparisons at observation point $k_{obs}$ over frequency band $[20, 2000]Hz$: confidence region prediction in dB with the probabilistic numerical model (gray region), numerical prediction in dB of the mean model (thick solid line) and experimental graphs of $f \mapsto \operatorname{Max}_{k_{obs}}^{\exp}(f)$ (upper thin solid line) and $f \mapsto \operatorname{Min}_{k_{obs}}^{\exp}(f)$ (lower thin solid line).

FIG. 9. Experimental comparisons at observation point $k_{obs}$ over frequency band $[20, 1000]Hz$: confidence region prediction in dB with the probabilistic numerical model (gray region), numerical prediction in dB of the mean model (thick solid line) and experimental graphs of $f \mapsto \operatorname{Max}_{k_{obs}}^{\exp}(f)$ (upper thin solid line) and $f \mapsto \operatorname{Min}_{k_{obs}}^{\exp}(f)$ (lower thin solid line).

$k_{obs}$

$k_{exit}$

0.60 m

PLATE P$_1$    JUNCTION    PLATE P$_3$
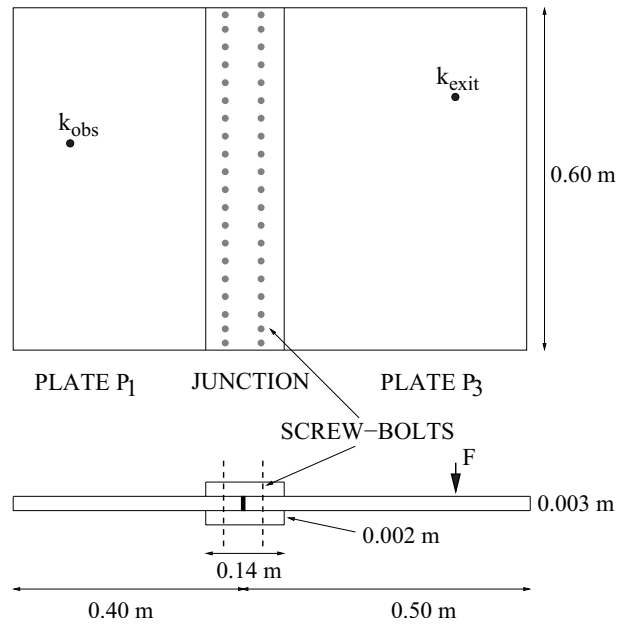
SCREW−BOLTS

F

0.003 m

0.002 m

0.14 m

0.40 m    0.50 m

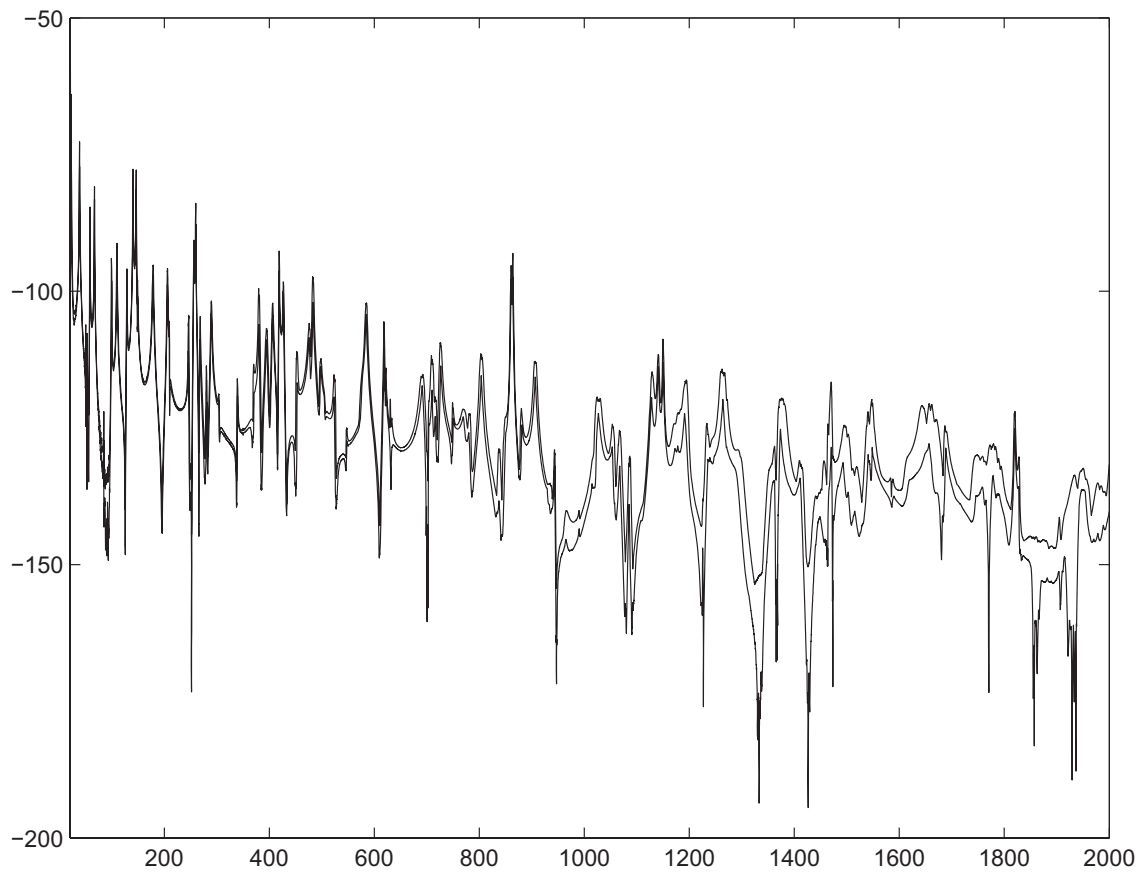Fig. 1, Hamid Chebli & Christian Soize, J. Acoust. Soc. Am.

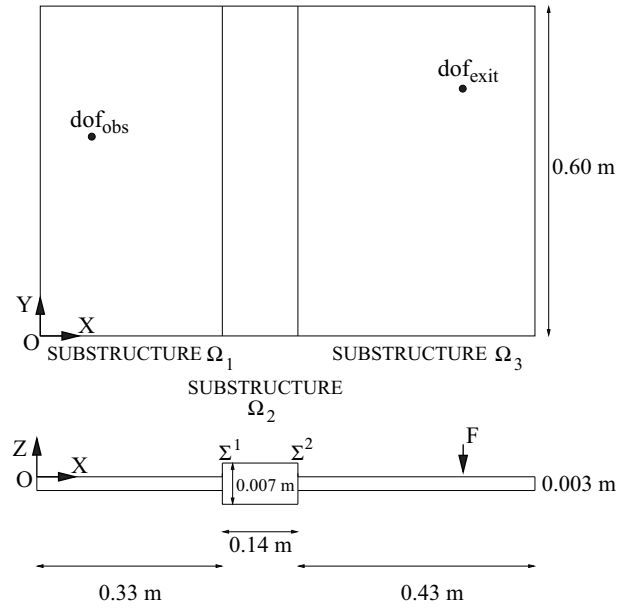Fig. 2, H. Hamid Chebli & Christian Soize, J. Acoust. Soc. Am.

Fig. 3, Hamid Chebli & Christian Soize, J. Acoust. Soc. Am.

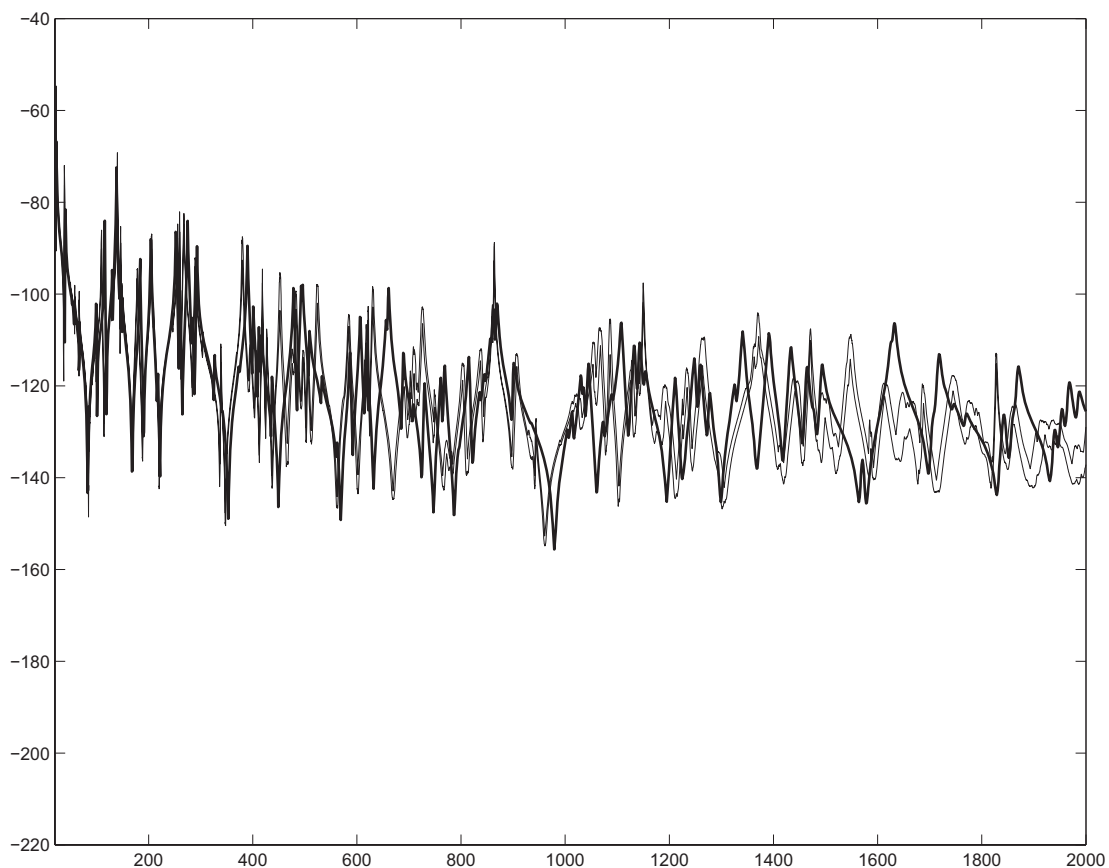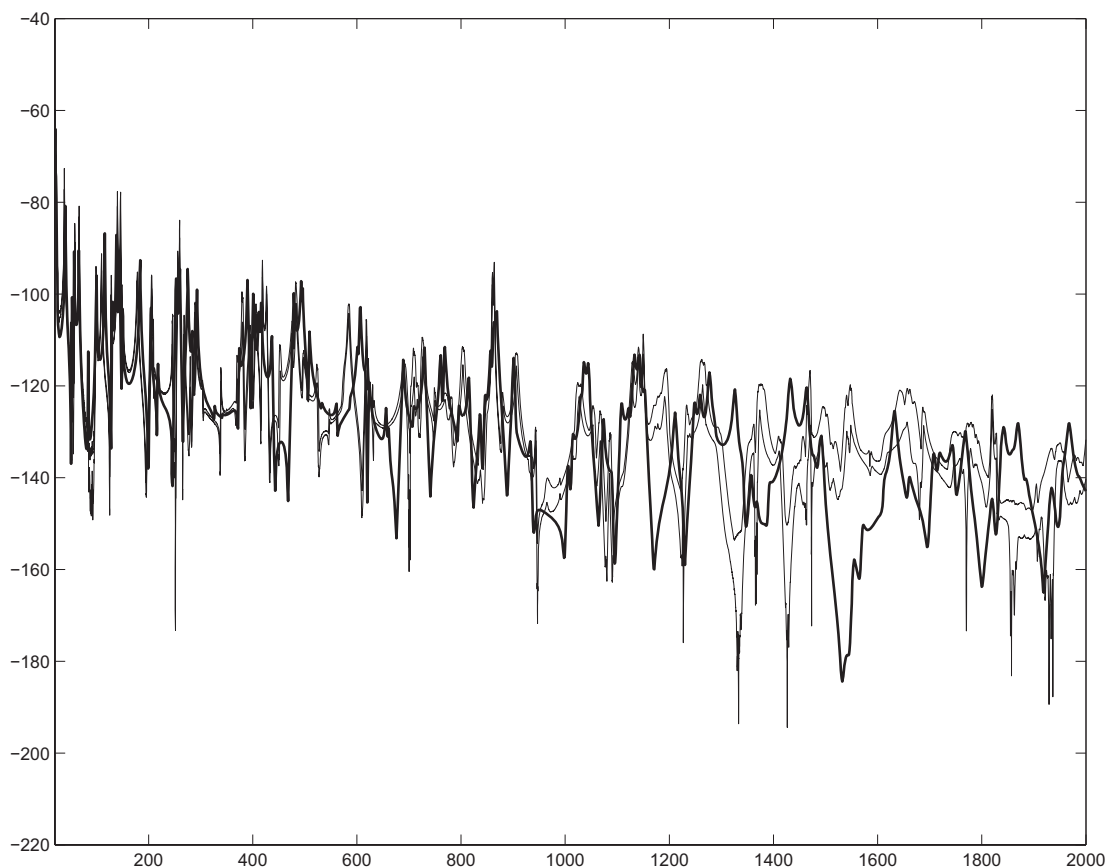Fig. 4, Hamid Chebli & Christian Soize, J. Acoust. Soc. Am.

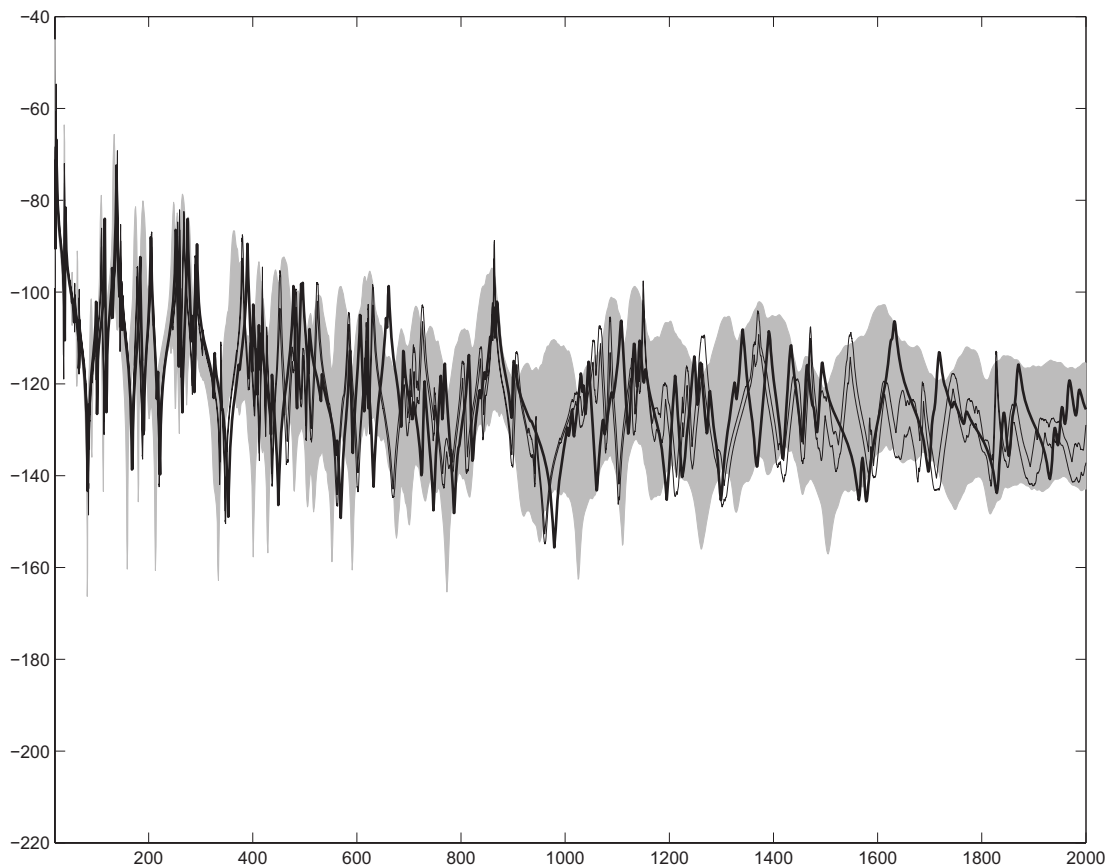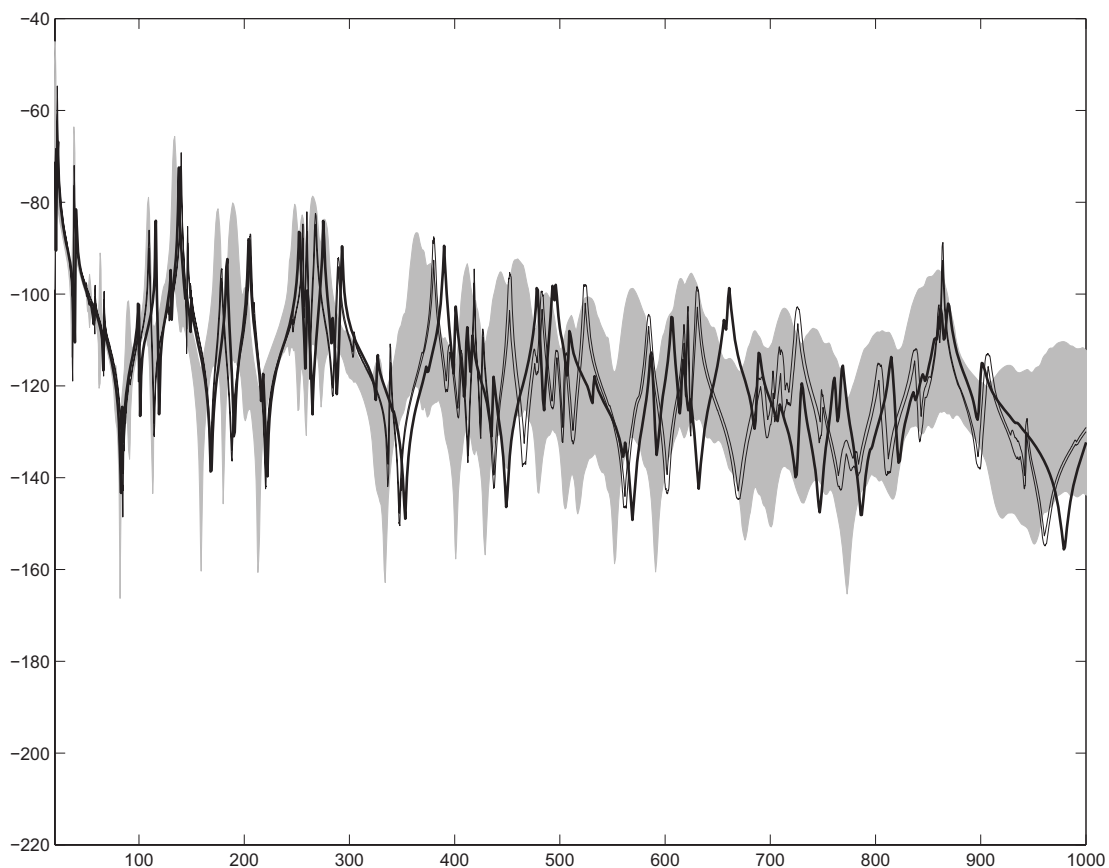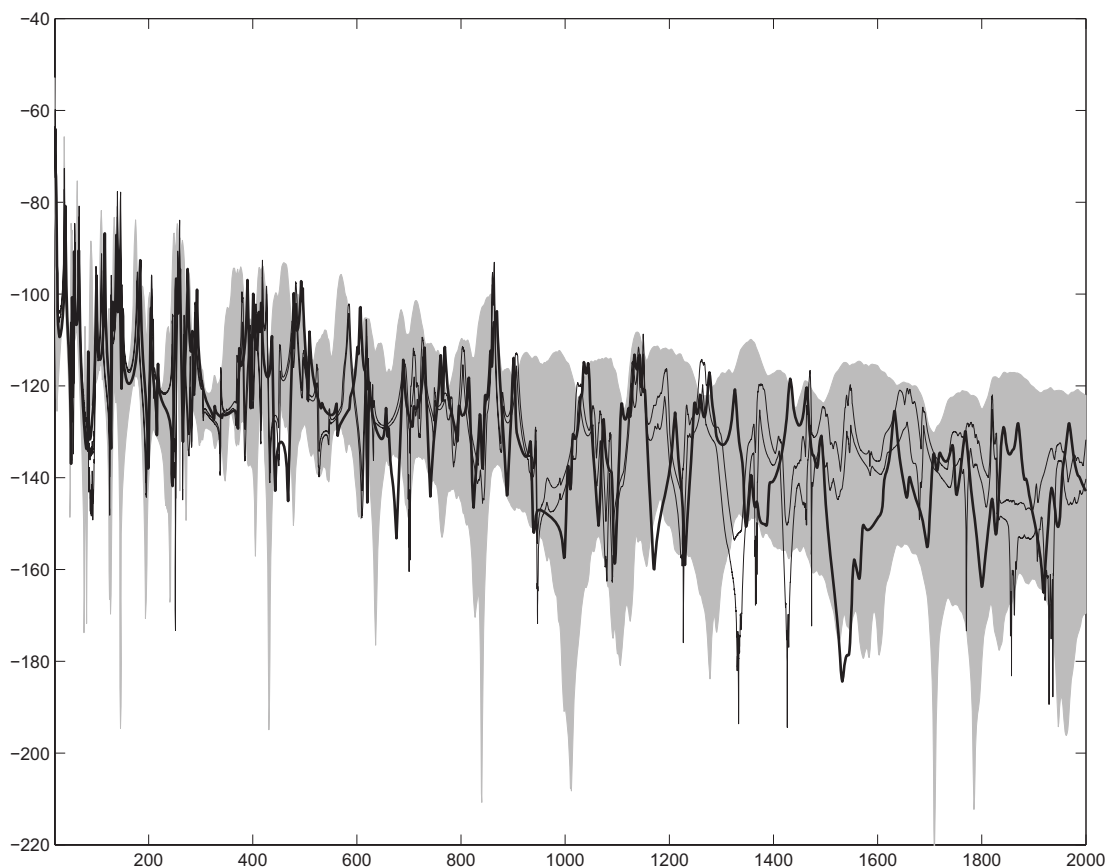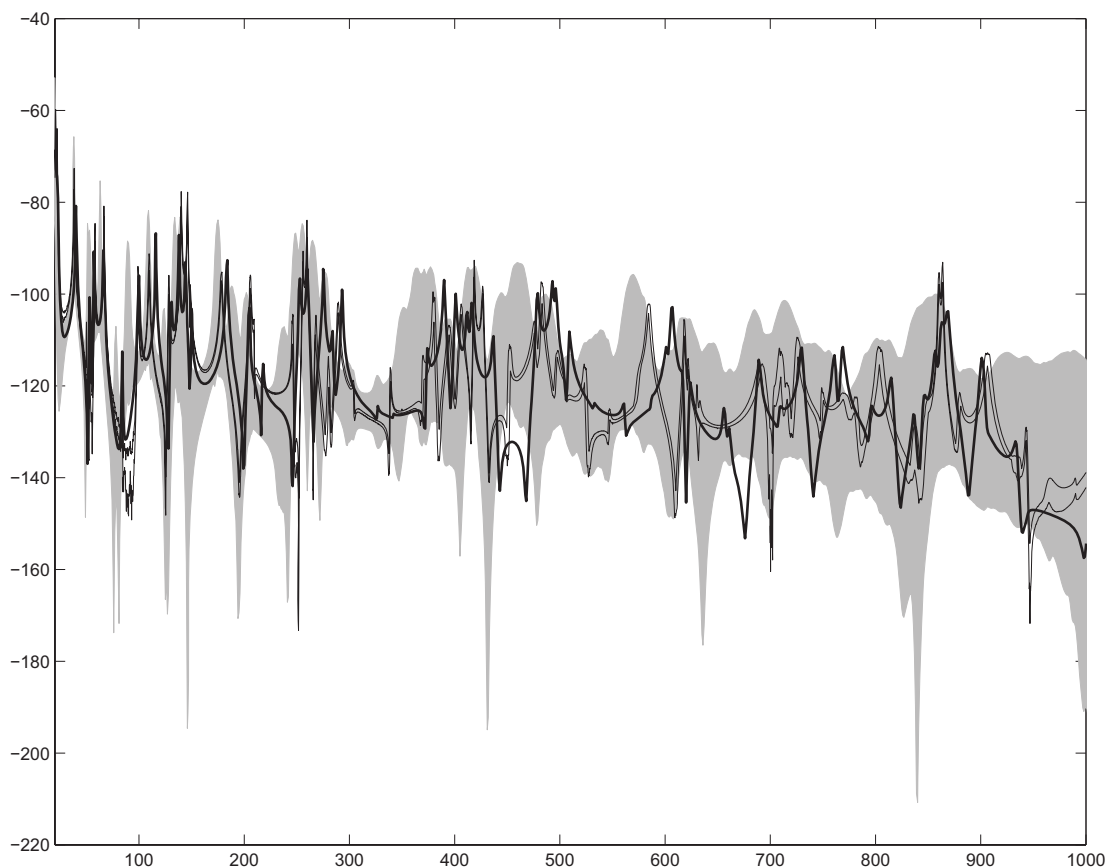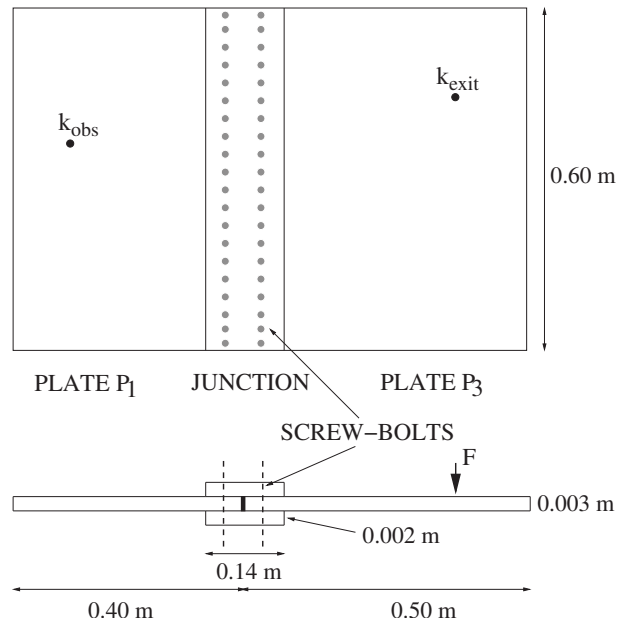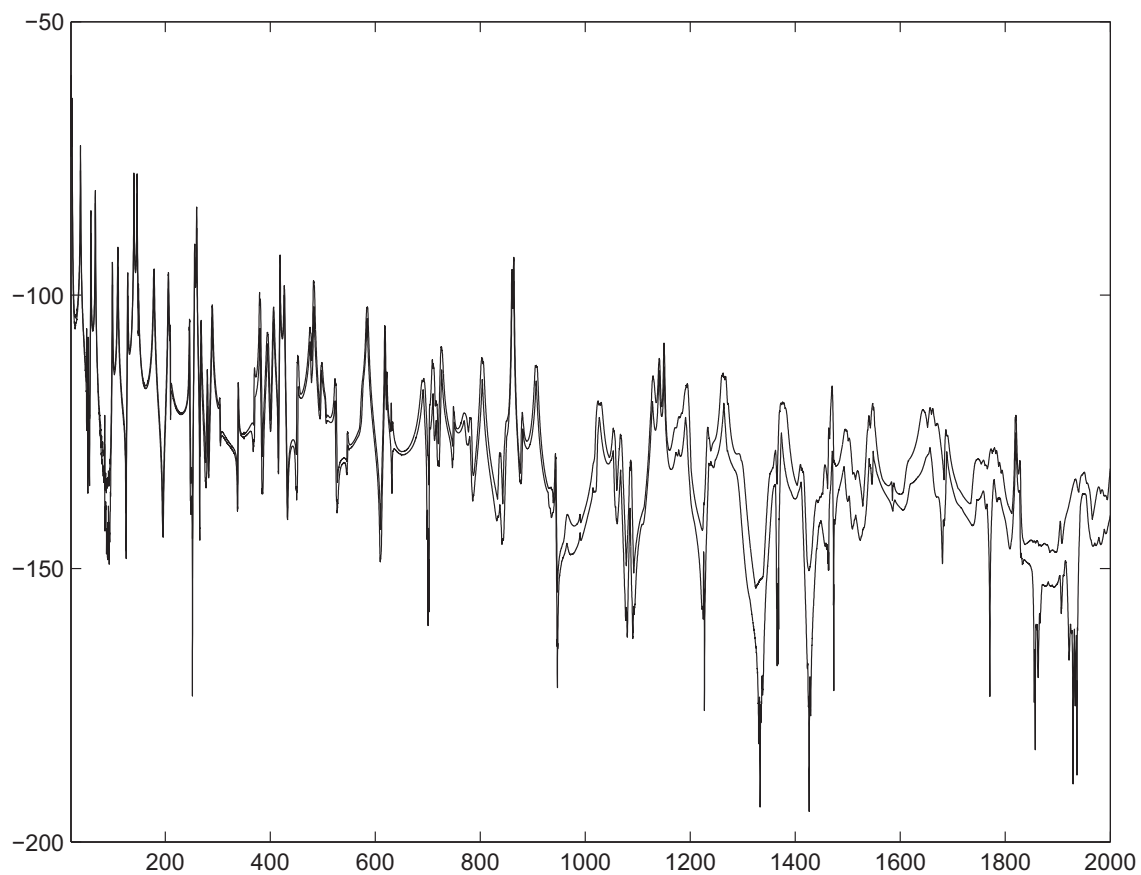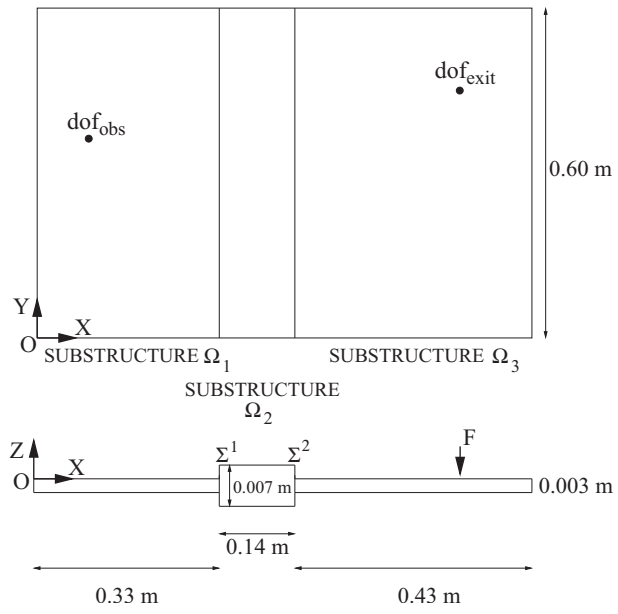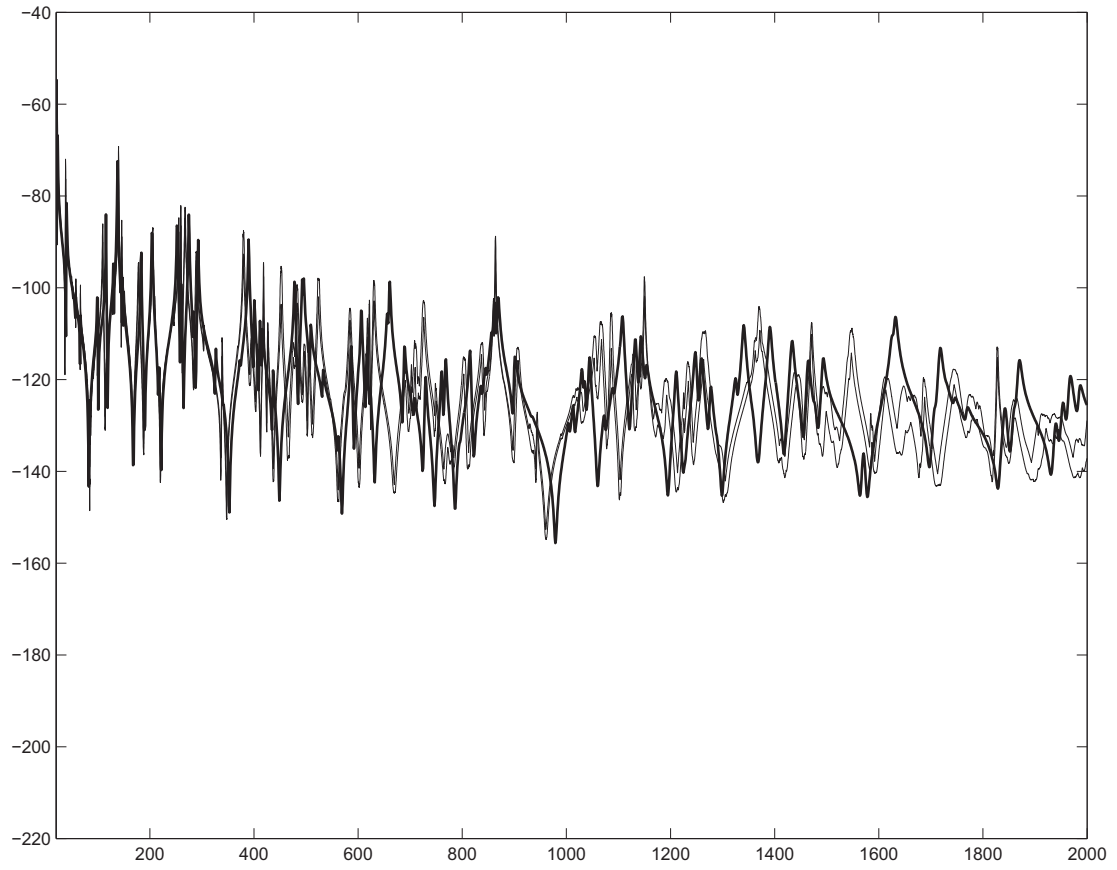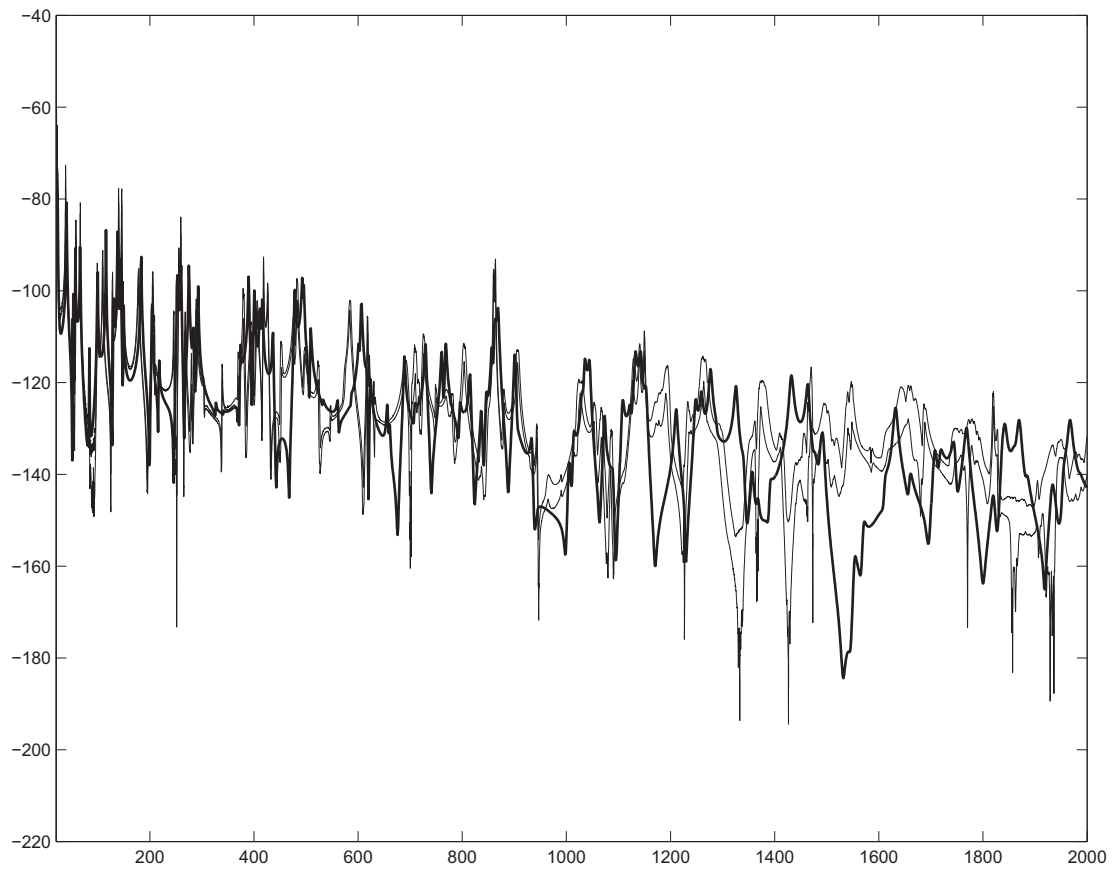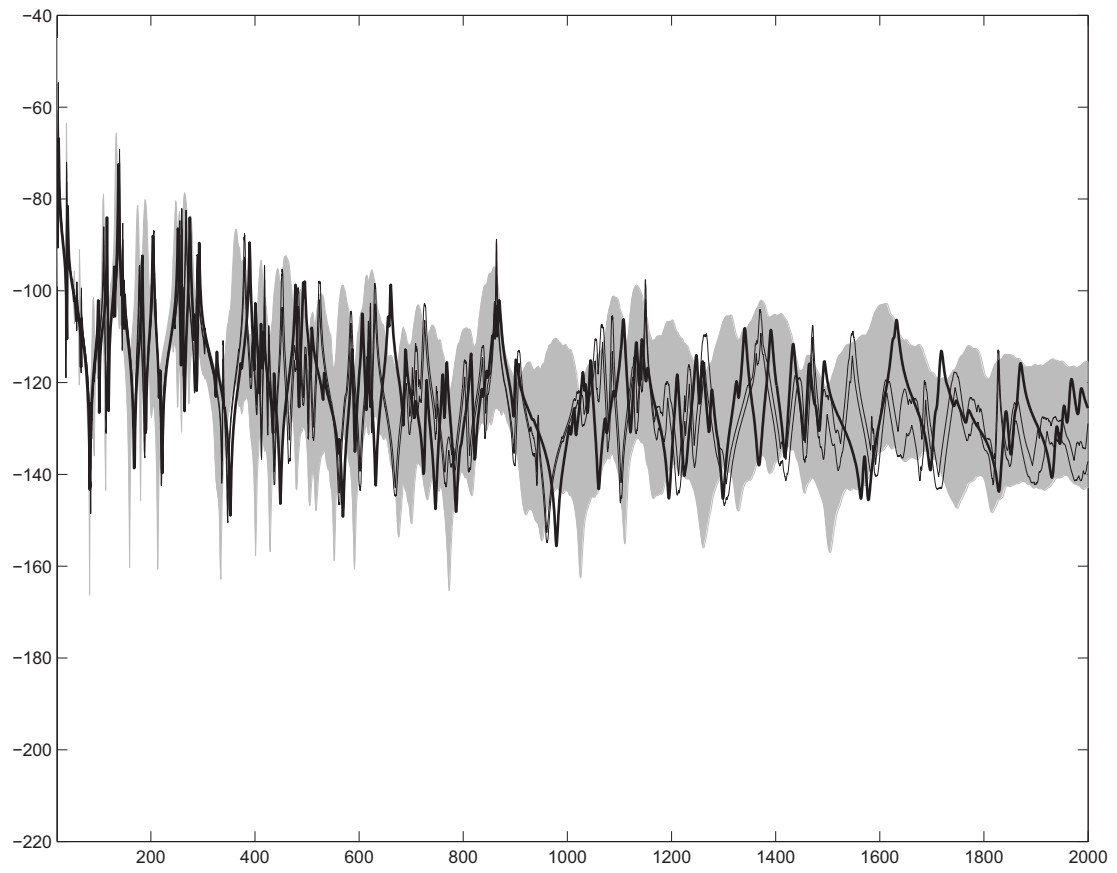Fig. 5, Hamid Chebli & Christian Soize, J. Acoust. Soc. Am.

Fig. 6, Hamid Chebli & Christian Soize, J. Acoust. Soc. Am.

Fig. 7, Hamid Chebli & Christian Soize, J. Acoust. Soc. Am.

Fig. 8, Hamid Chebli & Christian Soize, J. Acoust. Soc. Am.

Fig. 9, Hamid Chebli & Christian Soize, J. Acoust. Soc. Am.
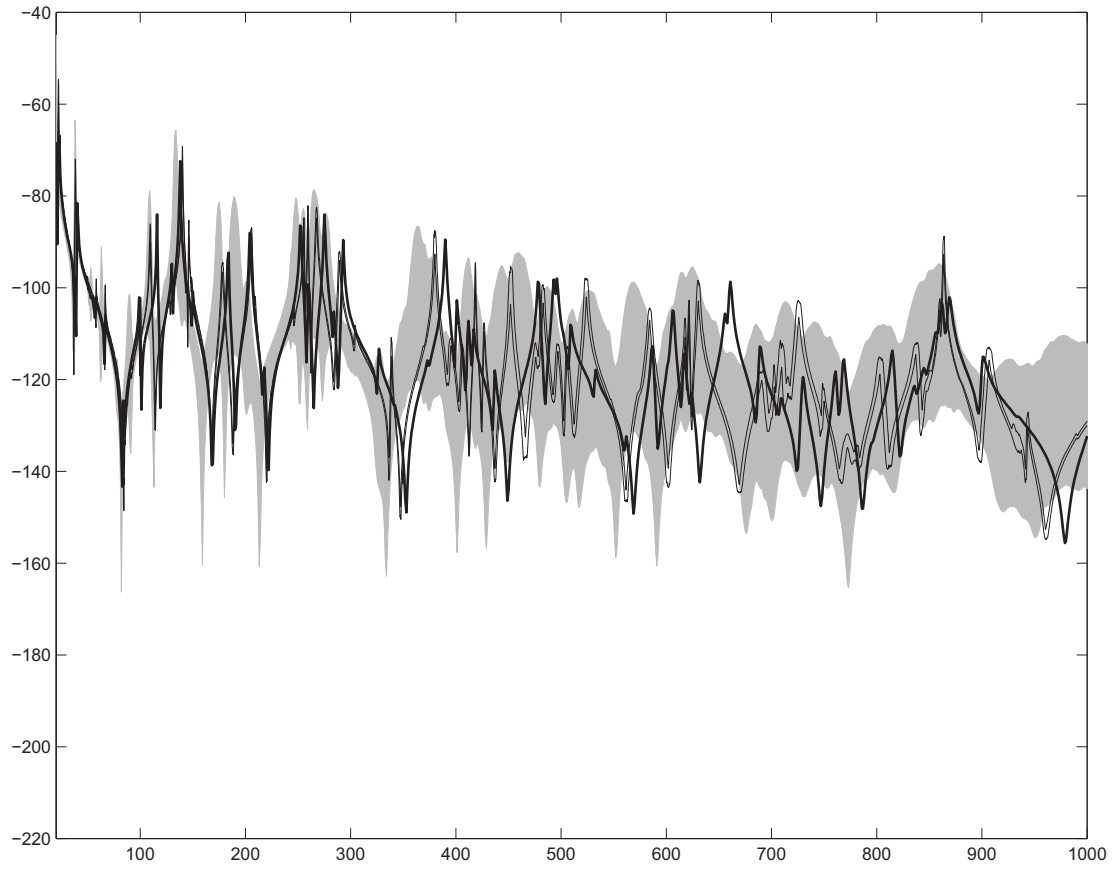
PLATE P$_1$          JUNCTION          PLATE P$_3$

k$_{obs}$

k$_{exit}$

0.60 m

SCREW−BOLTS

F

0.003 m

0.002 m

0.14 m

0.40 m

0.50 m

Fig. 1, Hamid Chebli & Christian Soize, J. Acoust. Soc. Am.

Fig. 2, H. Hamid Chebli & Christian Soize, J. Acoust. Soc. Am.

Fig. 3, Hamid Chebli & Christian Soize, J. Acoust. Soc. Am.

Fig. 4, Hamid Chebli & Christian Soize, J. Acoust. Soc. Am.

Fig. 5, Hamid Chebli & Christian Soize, J. Acoust. Soc. Am.

Fig. 6, Hamid Chebli & Christian Soize, J. Acoust. Soc. Am.

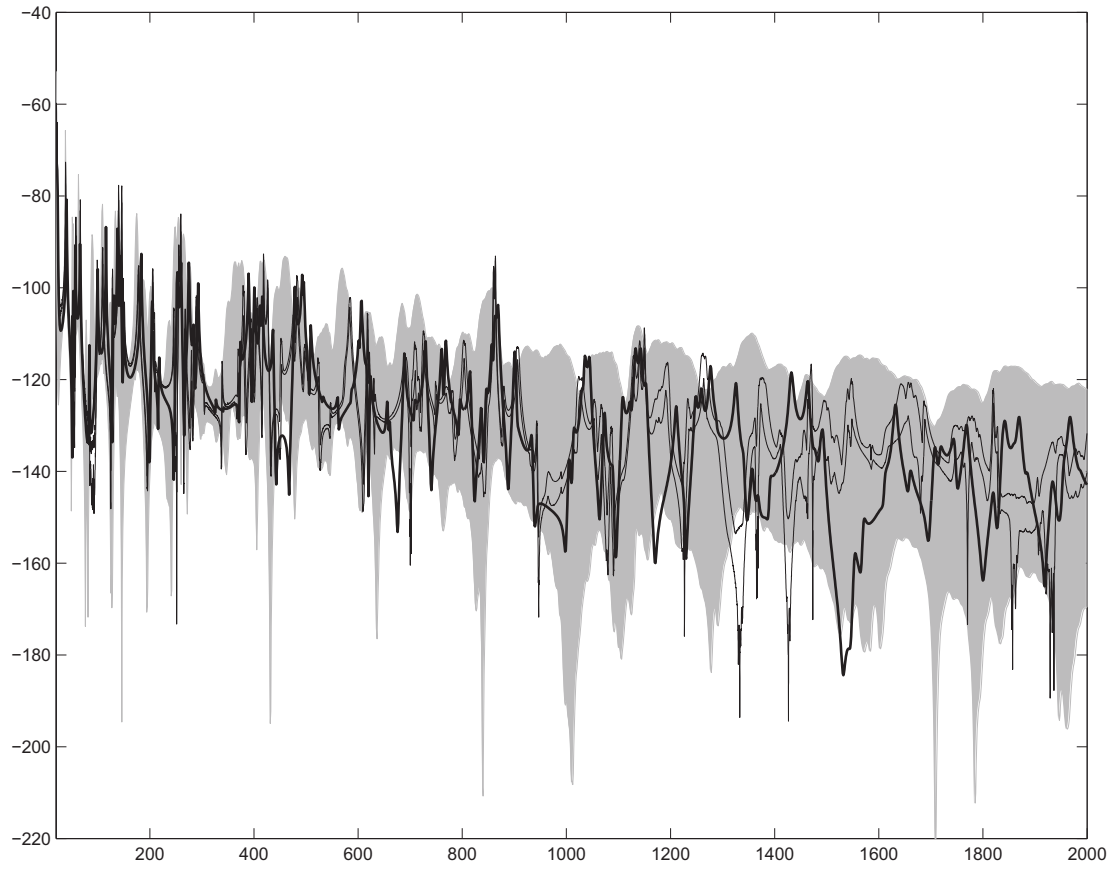Fig. 7, Hamid Chebli & Christian Soize, J. Acoust. Soc. Am.
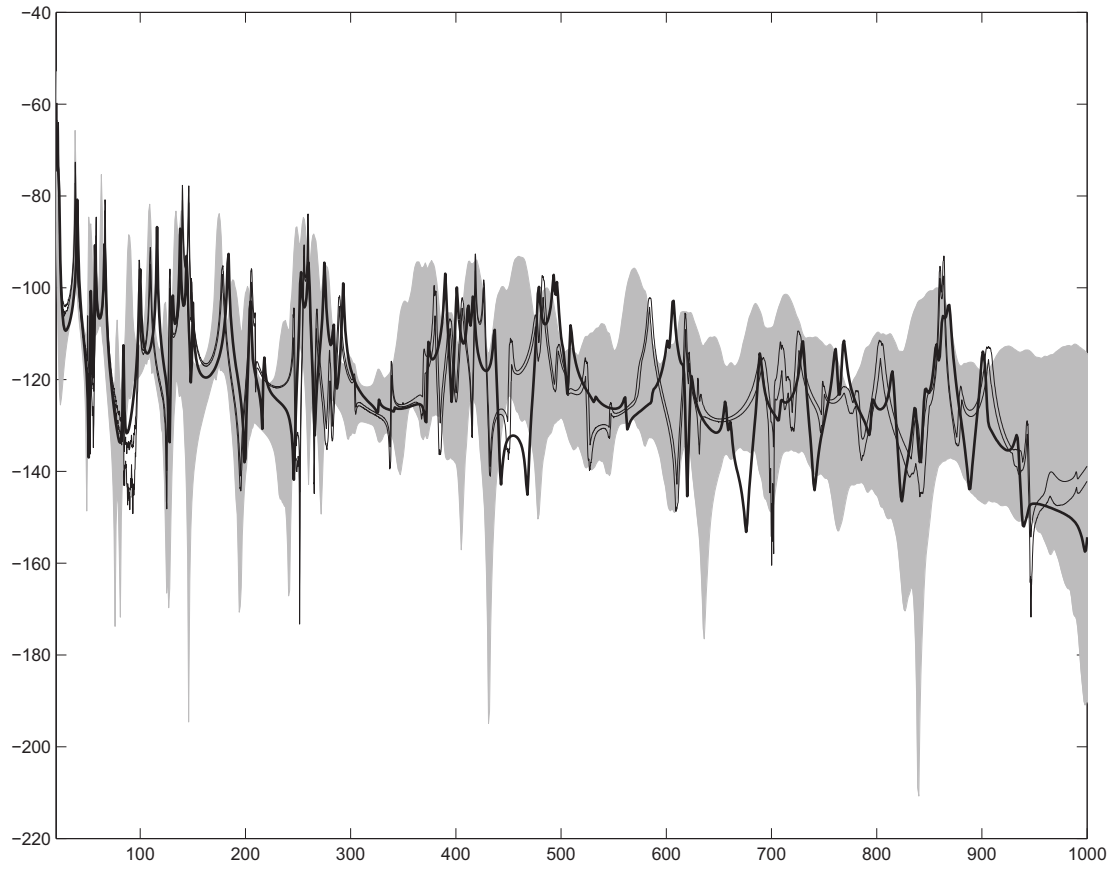
Fig. 8, Hamid Chebli & Christian Soize, J. Acoust. Soc. Am.

Fig. 9, Hamid Chebli & Christian Soize, J. Acoust. Soc. Am.